The In-flight icing warning system ADWICE for European airspace – Current structure, recent improvements and verification results

Frank Kalinka[1*], Katharina Roloff[2], Jakob Tendel[2] and Thomas Hauf[2]

[1]Deutscher Wetterdienst, Offenbach, Germany
[2]Institute of Meteorology and Climatology, Gottfried Wilhelm Leibniz Universität Hannover, Germany

Abstract

The Advanced Diagnosis and Warning System for Aircraft Icing Environments (ADWICE) has been in development since 1998 in a collaboration between the German Aerospace Centre (DLR), Deutscher Wetterdienst (German Weather Service, DWD) and the Institute of Meteorology and Climatology of the Leibniz Universität Hannover (IMuK). ADWICE identifies atmospheric regions containing supercooled liquid water where aircraft icing can occur. Running operationally at DWD since 2002, ADWICE is used at the German Advisory Centres for Aviation (Luftfahrtberatungszentrale) to support pilots in route planning by warning of hazardous in-flight icing conditions. The model domain covers Europe and the Mediterranean coast of North Africa with a horizontal grid spacing of about 7 km and 30 vertical hybrid levels. The warning system consists of two algorithms. Based on output data of the operational numerical weather prediction model COSMO-EU (Consortium of Small-Scale Modelling – Europe), the Prognostic Icing Algorithm (PIA) allows the forecast of areas with an icing hazard. The Diagnostic Icing Algorithm (DIA) realises a fusion of forecast, observational and remote sensing data such as satellite data to describe the current icing hazard. Both algorithms create a three-dimensional icing product containing information about the likely icing scenario and its associated icing intensity. This paper describes the current structure of ADWICE, its output, as well as its diagnosis and forecast skill. For verification, the output of the two algorithms was compared with pilot observations over Europe. The results show satisfactory values for the probability of detection and the volume efficiency.

Keywords: ADWICE, In-flight Icing, icing intensity, supercooled liquid water, supercooled large droplets, METEOSAT second generation

1 Introduction

Aircraft in-flight icing belongs to one of the most dangerous aviation weather hazards. Based on the National Transportation Safety Board (NTSB) and Aviation Safety Reporting System (ASRS) databases, Green (2006), among others, reported 944 icing related accidents and incidents between 1978 and 2005 in the United States. Appiah-Kubi (2011) added 228 accidents and 30 incidents for the following years 2006 to 2010. The physical reason behind this hazard is the existence of cloud supercooled liquid water (SLW) in the temperature range between $0\,°C$ and $-40\,°C$. Liquid water of that temperature is in a physically metastable state and may freeze spontaneously upon contact with any solid body such as an aircraft. When flying through such conditions, ice accretes on the leading edges of aerodynamic surfaces, increasing the aircraft's drag and modifying the flow and pressure distribution around the fuselage and, most importantly, the wing and tail. Depending on the amount of accreted ice, the aircraft performance degrades as long as the accreted ice is not removed. Details

of performance degradation were investigated, e.g., by Politovich (1996). Current appropriate de-icing systems are inflatable rubber boots or heated surfaces at the leading edge of a wing or at any other similar parts of the aircraft where the air stagnates and ice accretion is strongest. Clouds at sub-zero temperatures may exist as pure ice clouds such as cirrus clouds, pure liquid clouds, such as those found in the tropics ("warm clouds"), and in freezing fog, or as mixed phase clouds. In the latter case, both water phases exist simultaneously.

The creation of empirically based expert systems to diagnose and forecast aircraft icing was motivated by the aviation community's need to have accurate, non-text-based, colour coded graphical representations of icing hazards with the highest spatial and temporal resolution currently possible. The difficulty of simulating the formation processes with current numerical weather prediction (NWP) models arises from their small scale and the only meta-stable state of SLW clouds, which may remain in the liquid state for up to days in the absence of ice nuclei. These clouds can glaciate within minutes once nuclei are introduced into the cloud. Accurate simulation of the complex processes would require explicitly-solving cloud-microphysical interactions, as well as the complete knowledge of the initial conditions.

*Corresponding author: Frank Kalinka, Deutscher Wetterdienst, Research and Development Division, Frankfurter Strasse 135, 63067 Offenbach, Germany, e-mail: Frank.Kalinka@dwd.de

These requirements exceed the state of the art in modelling of processes, computing resources, and large-area measurements of the cloud microphysical state. These hard constraints are somewhat compensated by the icing expert systems using sufficiently reliable empirical relationships between observable meteorological quantities and icing severity. Empirical methods can be enriched with outputs from NWP models in a hybrid approach.

2 State of the art

To completely understand and eventually also model the in-flight icing process for the purpose of warning, two major problems have to be faced. The first is related to the existence of SLW, and the corresponding absence of natural freezing, and the second relates to the impact and ice accretion processes.

Supercooled liquid cloud particles either freeze spontaneously at temperatures below −40 °C, in what is referred to as homogeneous freezing, or when an ice nucleus initiates the freezing process, which is referred to as inhomogeneous freezing. A huge variety of airborne particles (aerosols) can function as ice nuclei, but they represent only a small number fraction (∼ 0.1 %) of all aerosols. Mineral dust was found by PRUPPACHER and KLETT (1997), DEMOTT et al. (2003), HUNG et al. (2003), soot by ANDREAE and ROSENFELD (2008) and KÄRCHER et al. (2007), as well as crystalline salts by ABBATT et al. (2006), WISE et al. (2010), SHILLING et al. (2006), MARTIN (1998), and ZUBERI et al. (2002). Recently, the importance of biological aerosol particles was noted by CHRISTNER et al. (2008) and MÖHLER et al. (2007). Ice particles themselves may also act as ice nuclei. The ability of any one particle to act as an ice nucleus – the activation of an ice nucleus – depends mostly on the temperature. With decreasing temperature, more ice nuclei become activated. This temperature effect, together with the available water vapour in the atmosphere that diminishes with lower temperature, leads to an observed maximum of SLW within the range of −5 °C to −20 °C, while peaking at about −10 °C (KOROLEV et al. 2003). Due to the metastable state of SLW and the fact that existing ice particles may act as ice nuclei as well, the natural freezing of liquid cloud particles in growing clouds – the glaciation of a cloud – may happen within minutes. Simulating such a rapid phase change in a numerical model requires comprehensive knowledge of the ice nuclei distribution, their chemical nature and the respective activation temperature. Numerical studies by PHILLIPS et al. (2002), ROSENFELD and WOODLEY (2000), LOHMANN and DIEHL (2006), FLOSSMANN and WOBROCK (2010), MORRISON and PINTO (2005) as well as THOMPSON (2012) show the importance of detailed ice nuclei information and its strong impact on cloud development. DEMOTT et al. (2011) clearly emphasise that the current understanding of ice nuclei is far from sufficient.

The impact of SLW drops on an aircraft and the subsequent freezing, the second major simulation challenge, occurs mainly near stagnation points of the airflow. Due to their inertia, droplets are less able to follow the curved airflow around the fuselage, engines, propellers and other parts exposed to the flow, and consequently impinge on the aircraft. Due to the release of latent heat during the freezing process, large droplets remain in a semi-liquid state for up to a second. During that time, they are able to flow downstream until all heat is transferred to the air and aircraft structure, and the ambient temperature is reached. Obviously, for low temperatures or very small drops, freezing occurs more or less on impact to form rime icing. For higher temperatures or relatively larger drops, e.g., between −5 °C and −10 °C and drizzle droplets, so called clear run-back ice with flow streaks of up to one metre can be observed. A complete understanding of the impact and freezing problem thus requires knowledge of the collection efficiency of each part of the aircraft for an initially unknown ambient SLW droplet size distribution. Both the freezing process and the related local heat transfer must then be solved. Eventually, the run-back flow must be simulated. In addition, it should be noted that the ice accretion shapes modify the airflow and thus the collection process itself. This results in typical ice accretion shapes with fingers or mushroom-like structures. Furthermore, in mixed phase conditions, impinging solid ice particles may stick to the accreted ice instead of bouncing from the airfoil. The aforementioned problems are simulated by extensive numerical ice accretion codes such as NASA's LEWICE (RUFF and BERKOWITZ 1990), ONERA (HEDDE and GUFFOND 1995) and Bombardier Aerospace's CANICE (TRAN et al. 1995). The amount of accreted ice depends obviously on the spatial distribution of SLW along the aircraft trajectory. The longer a flight in a homogeneous SLW field, the more ice accretes. This applies to a straight and level flight, but also to a holding pattern within the same cloud. The empirical relationship between temperature, average SLW content and a droplet size distribution for a given flight distance is described by a set of two-dimensional closed graphs, referred to as envelopes (Appendix C to Federal Aviation Administration (FAA) document 14 Code of Federal Regulations (CFR) Part 25 and 14 CFR Part 29) and is used for FAA aircraft certification (JECK 2002). The droplet size distribution is usually described by a single parameter such as the mean-volume diameter. Data used in Appendix C dating back to 1940–1960 do not reflect the significance of supercooled large droplets (SLD), commonly also known as drizzle drops, with diameters ranging between 40 and 500 μm. These drops especially contribute to the above mentioned run-back ice on the wing, and were determined to have contributed to some major accidents, among them the one in Roselawn (Indiana) in 1994 (MARWITZ et al. 1997). In the aftermath of that latter accident, a revision of Appendix C was initiated which resulted in new certification procedures and

guidelines. A complete revision of Appendix C, following the suggestions by COBER and ISAAC (2012), however, is still underway.

In summary, modelling of the complete in-flight icing process, especially for warning and route planning, including the ice accretion process, is beyond current capabilities and is therefore not currently feasible. Knowledge of aircraft icing situations and associated weather conditions are mainly based on pilot reports (PIREP) of aircraft icing encounters, about which numerous studies exist. TAFFERNER et al. (2003) explained the reasoning for the icing warning system and listed icing observations, similar to BERNSTEIN et al. (1997). POLITOVICH et al. (2002) investigated aircraft icing in winter storms over Colorado. BERNSTEIN et al. (2007) and BERNSTEIN and LEBOT (2009) inferred the existence of SLW, SLD and icing conditions from surface observations, temperature and moisture profiles. ROSENFELD et al. (2013) studied freezing drizzle in coastal areas of the Western US. POLITOVICH and BERNSTEIN (1995), as well as RASMUSSEN et al. (1995), deepened the understanding for the occurrence of aircraft icing in case studies. MARWITZ et al. (1997) examined icing-related aircraft accidents. Research flights in icing conditions including SLD focused on icing in convective as well as stratiform clouds (RASMUSSEN et al. 1992; HAUF and SCHRÖDER 2006; MILLER et al. 1998; RYERSON et al. 2000; ISAAC et al. 2001). These and other studies laid the foundation for heuristic and empirically based icing analysis and forecasting algorithms like IIDA (Integrated Icing Diagnosis Algorithm) and IIFA (Integrated Icing Forecast Algorithm) at NCAR in 1998 (SCHULTZ and POLITOVICH 1992; MCDONOUGH and BERNSTEIN 1999; POLITOVICH 2000). Their warning products CIP (Current Icing Product) and FIP (Forecast Icing Product) have been continuously improved since then. These products provide two types of information: the spatial and temporal distribution of clouds with an icing hazard, as well as the expected strengths of icing and SLD. The algorithms may also be referred to as expert systems which combine satellite, radar, surface, lightning and PIREP observations with model output to create a detailed three-dimensional hourly diagnosis of the icing hazard. The latter is expressed as the potential for the existence of icing and SLD and can be understood as a probability forecast. For the forecast product, numerical model data replace observed data and thus enable the forecast of an icing hazard using a similar algorithm. TAFFERNER et al. (2003) adapted the NCAR/Research Applications Program (NCAR/RAP) icing algorithm by THOMPSON et al. (1997) to Central European conditions and created the ADWICE warning system. The difference between the American and the German system originates from the different set of data sources and their qualities. One major difference in data quality is the denser network of surface observation stations in Europe (LEIFELD 2003). LEBOT (2003) has developed a similar type of icing warning algorithm SIGMA (System of Icing Geographic Identification in Meteorology for Avia-

tion) using available observational data at Météo France. SIGMA combines model, satellite and radar data every 15 minutes to diagnose the icing hazard for France and its bordering regions.

All these expert systems are affected by an over-forecasting and over-diagnosis of icing conditions as TAFFERNER et al. (2003), BERNSTEIN et al. (2005), TENDEL and WOLFF (2011) and TENDEL (2013) have proven during different verification studies. This is one reason for the continuous effort to adapt aircraft icing warning systems to new observational data sources. In 2014, the use of MSG satellite data was implemented into the diagnostic part of the German warning system ADWICE. This paper describes the current model structure and the implementation of satellite data into the algorithm. Furthermore, a case study will show an improvement of the diagnosing skill of ADWICE, which can be traced back to the implementation of satellite data.

3 Current model structure

TAFFERNER et al. (2003) described the structure of the ADWICE algorithm which was developed initially for diagnostic purposes by using observational data, among other data sources. Since then, two major changes were made in the system structure. For the operational use of ADWICE within the DWD, it was on the one hand indispensable to extend the algorithm by a prognostic part (LEIFELD 2003). Especially at the German Advisory Centres for Aviation, forecasts of icing conditions were necessary for supporting pilots in planning icing-free flight paths some hours before take-off. On the other hand, the remaining diagnostic part of the algorithm was adapted to the new observational data source provided by satellites (TENDEL 2013). The current model structure is presented in the following sections.

3.1 Input data from COSMO-EU

Both the diagnostic and the prognostic part of ADWICE depend on input data from a NWP model which is currently provided by the German mesoscale model COSMO-EU (formerly Lokalmodell). COSMO-EU is a non-hydrostatic compressible NWP model with a rotated grid and a horizontal resolution of about 7 km (DOMS 2011). For simplifying the post-processing of NWP data in ADWICE, the grid structure of COSMO-EU was transferred into ADWICE. However, only the lower 30 vertical hybrid levels of COSMO-EU are used for deriving icing warnings in ADWICE, due to the fact that in the upper ten levels, the temperature is too low for the existence of SLW.

For parameterising cloud microphysical processes, a one-moment bulk model is implemented in the model physics. With the aid of a two-category ice scheme, the evolution of the microphysical classes of cloud water, cloud ice, rain, snow and water vapour are modelled. Whereas the total mass fraction of each class is predicted directly by COSMO-EU, the size distributions
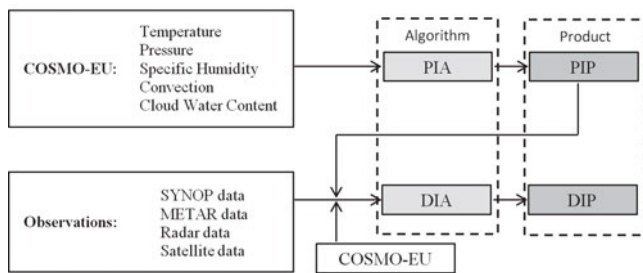
Figure 1: Algorithm structure of the German aircraft icing warning system ADWICE: the Prognostic Icing Product PIP is generated by running the PIA-algorithm with COSMO-EU data as input data. The combination of PIP, observations and model data in the DIA-algorithm results in the Diagnostic Icing Product DIP.

Figure 2: Vertical profile of temperature and dewpoint temperature for which PIA identifies the icing scenarios "Freezing" (red) and "General" (blue).

of the particles are assumed to be monodisperse for the non-precipitating classes, and exponentially distributed with respect to the hydrometeor diameter for the precipitating classes (DOMS et al. 2011). Furthermore, neither the transport nor the chemical composition of ice nuclei are implemented in the parameterisation of cloud microphysical processes; just a temperature dependent ice nuclei concentration is included. Therefore, a satisfactory description of the inhomogeneous freezing process as well as the amount and spatial distribution of liquid water content cannot be supplied currently by COSMO-EU (ROLOFF 2012; KÖHLER and GÖRSDORF 2014).

3.2   Algorithm to forecast icing conditions

The Prognostic Icing Algorithm PIA receives COSMO-EU input data as illustrated in Figure 1. The forecast profiles of temperature and specific humidity are scanned by PIA to distinguish between four different icing scenarios resulting in the Prognostic Icing Product (PIP), as will be explained in the following subsections. The thresholds for temperature and humidity required by these scenarios were originally derived for the IIDA algorithm and were based on observational data in the vicinity of icing PIREPs (THOMPSON et al. 1997; SCHULTZ and POLITOVICH 1992). They later were adapted to European conditions by LEIFELD (2003). The classification into four icing scenarios reflects the expected droplet sizes within the predicted icing areas, including SLD. After identifying the relevant specific scenario, the associated icing intensity is derived from meteorological parameters. A detailed description of this calculation is given in Section 3.4.

3.2.1   Scenario "Freezing"

The icing scenario "Freezing" was implemented in PIA to describe a major hazard of icing conditions associated with supercooled drizzle and rain drops generated by a subfreezing air mass below a melting layer only. Those specific SLD conditions may be observed both at ground level and aloft. A typical vertical profile of the temperature and dew-point temperature is shown in Figure 2. During these conditions, it is assumed that solid
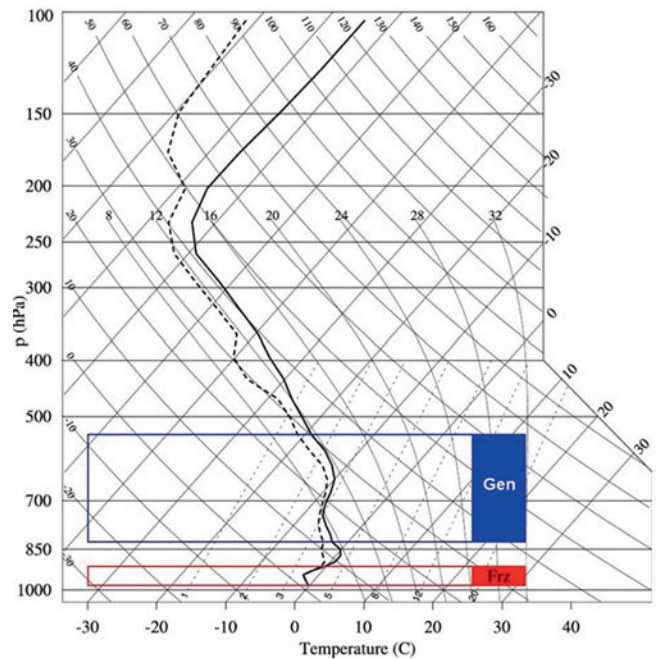
precipitation falls into a temperature melting layer that is above 0 °C, referred to as a so-called warm nose in the temperature profile. If the vertical extent of the melting layer is sufficient, the solid particles will fully melt and form drizzle or rain drops. Below the melting layer, a subfreezing air mass leads to supercooling of the falling drops. In the absence of collisions with ice nuclei or newly generated cloud ice particles, the drops remain liquid at temperatures below freezing point.

For identifying the scenario "Freezing", PIA analyses the temperature and humidity profile from the surface up to the 30th model layer. At first, a low-level subfreezing layer ($T < 0$ °C) must be detected. Next, the lower and upper boundaries of the warm nose are determined with above zero temperatures in between. Finally, a precipitating cloud with a vertical extent of at least 3000 m has to be present above the warm nose, identified solely from temperature and humidity data. The relative humidity (derived from the specific humidity) is used as a cloud indicator, assuming that the relative humidity must be higher than 80 % in the precipitating cloud. A dry air mass with a vertical extent of greater than 3000 m between the cloud base and warm nose is assumed to result in total evaporation of ice crystals and no resulting melted precipitation.

If the latter conditions are all met by PIA, the scenario "Freezing" is assigned to all layers below the warm nose with a temperature between −20 °C and 0 °C.

3.2.2   Scenario "Stratiform"

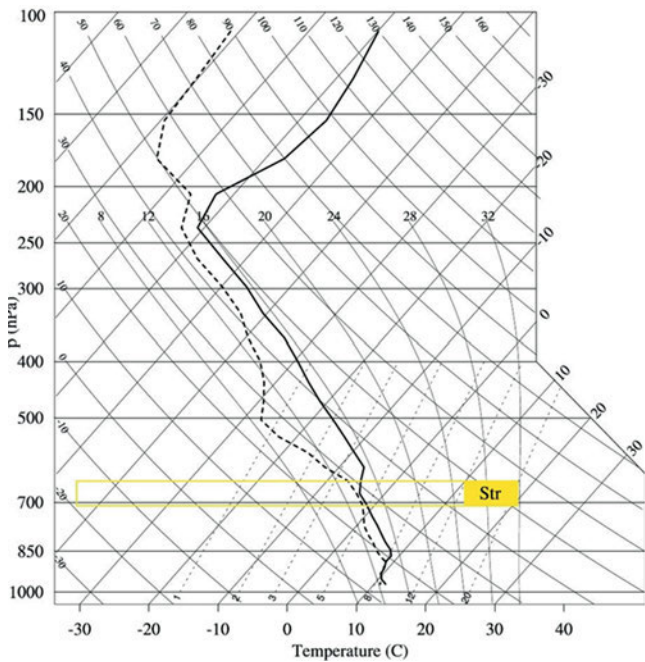The scenario "Stratiform" describes freezing drizzle conditions within inversion capped sub-zero stratiform

Figure 3: Vertical profile of temperature and dewpoint temperature for which PIA identifies the icing scenario "Stratiform" (yellow).
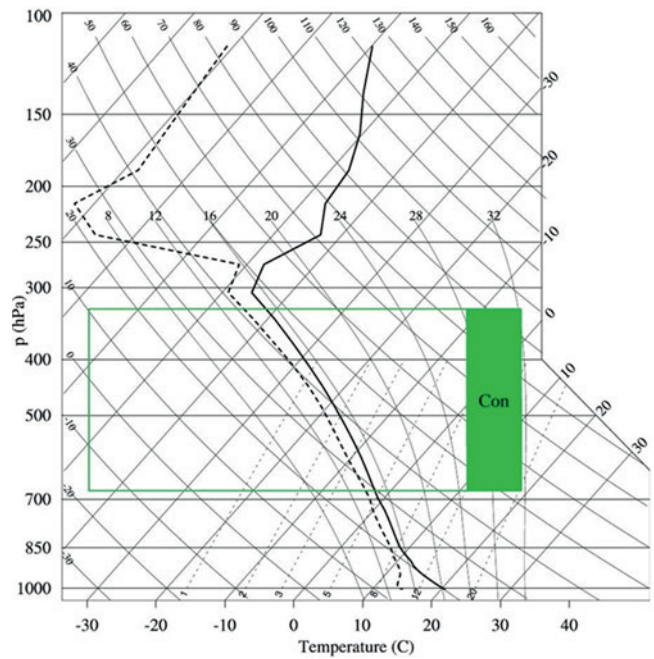

Figure 4: Vertical profile of temperature and dewpoint temperature for which PIA identifies the icing scenario "Convective" (green).

clouds where the collision-coalescence process dominates droplet growth. The hazard for aviation results from the possible occurrence of SLD and the occasionally huge horizontal extent of these stratiform cloud layers. For identifying this scenario, PIA initially tries to detect a moist, subfreezing cloud layer with temperatures between −12 °C and 0 °C (Cober and Isaac 2012) and a relative humidity of not less than 80 %. A characteristic gradient in relative humidity of at least −2.5 % per 100 m is interpreted as the top of the stratiform cloud layer. Finally, it has to be checked whether there is a precipitating cloud above this stratiform layer which could deplete the supercooled droplets by inserting ice particles. To exclude this glaciation process, the distance between the stratiform cloud top and a potential precipitating cloud base aloft has to be greater than 3000 m. If these conditions are identified by PIA, all layers below the characteristic humidity gradient with a temperature between −12 °C and 0 °C are assigned with the scenario "Stratiform" (see also Figure 3).

3.2.3 Scenario "Convective"

The icing scenario "Convective" describes icing conditions in convective cloud systems that are related to their strong updraughts and condensation processes resulting from adiabatic cooling of lifted air masses. Huge amounts of SLW can rapidly be transported to great heights until homogeneous freezing starts at temperatures below −40 °C. The existence of SLD in convective clouds is therefore likely, especially in deep convective clouds. Because of its resolution of about 7 km, COSMO-EU cannot resolve convective cells to scale. Hence, a mass flux scheme is needed. The implemented

Tiedtke (1989) scheme parameterises sub-grid scale convection within the model and provides the convective cloud top z_{top} and cloud base z_{base} for each COSMO-EU grid point. Taking these values, PIA calculates the vertical extent of the convective clouds

$$\Delta z_{conv} = z_{top} - z_{base}. \qquad (3.1)$$

If that convection depth is greater or equal to 3000 m and the temperature within the cloud is between −40 °C and 0 °C, all convective layers are assigned with the scenario "Convective". In Figure 4, an example is shown where the scenario "Convective" reached a vertical extent of about 4500 m. The minimum value of 3000 m for the convective vertical depth was chosen to exclude shallow convection which does not generally pose a significant hazard to aviation.

3.2.4 Scenario "General"

The scenario "General" was implemented to describe cloud-droplet icing under less-specific atmospheric conditions than the other scenarios. It is only assigned to non-SLD clouds that have not previously been identified by one of the other scenarios, and whose temperature lies between −20 °C and 0 °C at an appropriate relative humidity. This threshold relative humidity is calculated by a linear function of temperature with a minimum value of 63 % at −20 °C and a maximum value of 82 % close to 0 °C. In nature, liquid clouds have a relative humidity close to 100 %. The lower humidity thresholds used in ADWICE were derived from a multitude of radiosonde observations in the vicinity of pilot reports of icing according to Forbes et al. (1993). They found a

mean relative humidity of 82 % with a standard deviation of 19 % (therefore the thresholds 63 % and 82 % in the algorithm). The scenario "General" is also applied to upper layers in multilayer icing conditions above one of the previously defined icing scenarios. Figure 2 shows such a multilayer situation with the scenario "Freezing" identified near the surface and the scenario "General" aloft. The precipitating cloud which is needed for the identification of the scenario "Freezing" is assigned with the icing scenario "General" in this case.

3.3   Algorithm to diagnose icing conditions

Icing forecasts based solely on humidity and temperature thresholds from model data (like in PIA) generally produce a high false alarm rate (TAFFERNER et al. 2003). This mainly is a result of the model's grid resolution, which is too coarse to resolve clouds correctly. Lower thresholds of relative humidity result in higher rates of false alarms (because of the overestimation of icing). Using a high threshold of relative humidity assumes that we rely on a numerical model to forecast clouds correctly. Therefore, the aim is to use thresholds that will lead to a high probability of detection and a low false alarm rate. THOMPSON et al. (1997) did not succeed in tuning relative humidity, and therefore suggested to use icing predictions as a first guess and improve it by using additional data from satellites, synoptical stations (SYNOP) or RADAR. In the Diagnostic Icing Algorithm (DIA) of ADWICE, the model-based PIP described in Section 3.2 is therefore initially used as a first guess of icing conditions. To minimise a possibly high false alarm rate, assigned icing scenarios of PIP are confirmed, extended or rejected by surface observations from SYNOP stations, METeorological Aerodrome Reports (METAR) and by remote sensing data from radar information. Nevertheless, there exists a lack of operationally available, widely distributed and systematic surface observations of vertical information about cloud ceiling, the temperature and the humidity profile. However, this information is necessary to find a possible melting layer as well as the vertical extent of a possible icing risk. Using additional remote sensing data sources that have become operational in recent years, the false alarm rate can be further reduced in many situations. Such satellite derived products are used in a further step for identifying (non) hazardous clouds and for determining their vertical extent. In the current Diagnostic Icing Algorithm (DIA), operated by DWD, surface observations are still treated as the most direct and reliable data sources, followed by remote sensing retrievals (radar, satellite data), followed by model data.

TAFFERNER et al. (2003) explicitly described the implementation of observation and radar data into DIA. Therefore, the following chapter will mainly focus on a detailed explanation of the integration of satellite data and only briefly describe the fusion of synoptic and radar data.

3.3.1   Synoptic data

According to BERNSTEIN and LEBOT (2009), there is a strong correlation between defined surface weather phenomena and the detection of supercooled droplets in clouds and precipitation. Cloud ceiling and cloud type as well as significant weather are reported by ground observations and provide a first guess, not only about the location of clouds, but also about their vertical dimension and the cloud phase. In accordance with the previously described four icing scenarios ("Stratiform", "Convective", "Freezing" and "General"), DIA tries to identify possible icing scenarios by using observed weather information from SYNOP and METAR reports. Shower and thunderstorms, for example, indicate a strong vertical development of clouds and, therefore, a likely existence of supercooled liquid droplets (scenario "Convective" confirmed). Drizzle is typically an indicator for a thin cloud layer and, therefore, possibly confirms the stratiform icing risk. Snowfall is a sign that icing conditions are likely non-existent as supercooled water does not persist in the presence of ice crystals because of riming and/or the Bergeron-Findeisen process (PRUPPACHER and KLETT 1997) (icing scenarios rejected). If freezing rain is observed at the surface, it is a direct proof of the existence of supercooled large droplets aloft between the ground and the melting layer and, therefore, the icing scenario "Freezing" is set or confirmed. Because weather reports by automatic stations still suffer from quality deficiencies, especially for freezing precipitation, only information from manned stations are currently used in DIA.

Weather observations are normally valid for the geographical location they are made, e.g., the precipitation amount. On the other hand, cloud observations refer to a larger area. In practice, the observed weather phenomenon is interpreted as a representative information source for a certain surrounding area. To define the validity area around an observation, the "Voronoi-Method" is applied (DEBERG et al. 2000) which subdivides the model domain into a honeycomb of polygonal cells, each with a weather station at its centre. The cell borders are drawn at the halfway point to neighbouring weather stations or at 70 km, whichever is closer. Every grid point of the model domain located in one such cell is associated with the observation value of the respective weather station. Further information about transferring spatial fixed weather observations to the ADWICE grid are found in LEIFELD (2003).

3.3.2   European radar composite

A radar reflectivity product from a Europe-wide weather radar network is used to detect possible icing risk areas. A reflectivity higher than 19 dBZ suggests a weather situation with rain or snowfall while values lower than 19 dBZ are typical for uniform stratiform clouds with echoes caused by drizzle, small rain droplets, or small snowflakes (scenario "Stratiform" confirmed). Radar data thus are helpful in identifying some current weather situations, including clouds with icing risk.
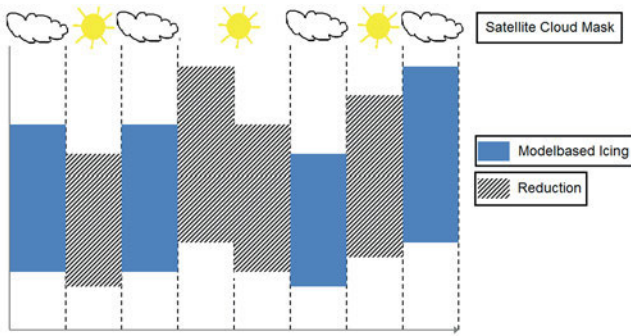
Figure 5: Usage of a satellite's Cloud Mask: Reduction of model-based icing columns by setting cloud free areas as icing free.

Figure 6: Reduction of model-based icing tops using satellite Cloud Top Height. CTH is compared with the model-derived top of icing, if present, and restricts the top of diagnosed icing at or below the satellite-derived CTH.

3.3.3 Satellite data

ADWICE-DIA is configured conservatively to prioritise minimum misses over false alarms. Incorrect non-warnings of icing conditions are seen as more harmful than false alarms. Therefore, some over-diagnosis of icing is expected. For the purposes of planning safe and efficient flights, operators of small general aviation aircraft require reliable guidance where non-icing conditions are expected. Therefore, the main achievement of implementing satellite based products into DIA was to increase the area where a confident no-icing diagnosis can be made. This was accomplished by substantially reducing the overall atmospheric volume of diagnosed icing while maintaining high diagnosis accuracy against positive icing reports.

Four different satellite based products, derived from METEOSAT 2nd generation (www.nwcsaf.org), have been implemented.

- *Cloud Mask*. Cloud Mask is a direct satellite product and distinguishes between cloudy and cloud-free atmospheric columns. Because icing conditions in cloud free areas on the order of a model grid box of 7 km × 7 km are expected to be unlikely, cloud free areas are set to "icing-free" (Figure 5). This product therefore represents a reduction in areas with an identified icing risk.
- *Cloud Top Temperature (CTT)*. CTT is a direct satellite product derived from the radiative brightness at the top of clouds. In relation to aircraft icing risk, it offers several indications whether icing can occur or not. If a specific cloud is well mixed and capped by an inversion layer and temperature increases from cloud top to cloud bottom (as generally in clouds), the minimum temperature of the cloud will be found in the cloud top. Therefore, if CTT is above the freezing point, no sub-zero temperatures are assumed within that cloud and any previously diagnosed icing within that column is removed. Since the identification of multilayer clouds based only on cloud-top products is currently inaccurate, the reduction of icing in multilayer cases can only be applied to the uppermost layer and allow no assumptions about lower cloud layers. Reduction of icing by CTT is there-
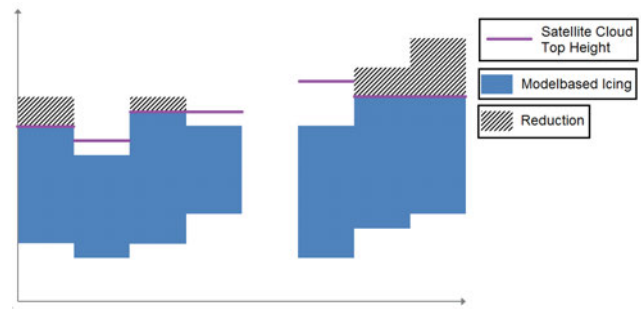
fore restricted to the clear case of satellite-measured above-freezing cloud-top temperature disagreeing with model-derived sub-freezing cloud tops.
- *Cloud-Top Height (CTH)*. CTH is indirectly derived from CTT by using a simulated vertical temperature profile to determine the geometric height of clouds. In DIA, satellite CTH is compared with the model-derived top of icing, if present, and restricts the top of diagnosed icing at or below the satellite-derived CTH (Figure 6). This leads again to a reduction in icing areas.
- *Cloud Phase*. Cloud Phase is a direct satellite product which differentiates between liquid water and ice at the cloud tops. In DIA, it is used in combination with Cloud Mask and CTT to add or confirm existing columns of icing at a height given by CTH. Since the ground observations provide information mainly about icing-relevant processes in the lowest cloud layer, the perspective on cloud-top conditions provided by satellite data may even be complementary to ground observations. This can be particularly useful in confirming or correcting the upper boundary of icing layers. Furthermore, complete reliance on model-based vertical profiles not supported by ground observations is seen as less reliable, and icing diagnosis in such cases can benefit from the direct input of satellite observation data. If there is a cloud whose phase is determined as liquid by the Cloud Phase product and if CTT is between 0 °C and −20 °C, a general icing risk is assigned to sub-freezing cloud layers up to 1000 m below the cloud top (Figure 7). The combination of CTT, CTH, Cloud Mask and Cloud Phase determines an addition and/or confirmation of icing.

Surface observations are always treated as the most direct and reliable data sources, followed by remote sensing retrieval (radar, satellite), followed by model data.

3.4 Calculation of icing intensity

After the detection of icing scenarios in PIA and DIA, an icing intensity value is calculated for each gridpoint with an assigned icing scenario. The icing intensity should correlate with the ice accretion rate on air-
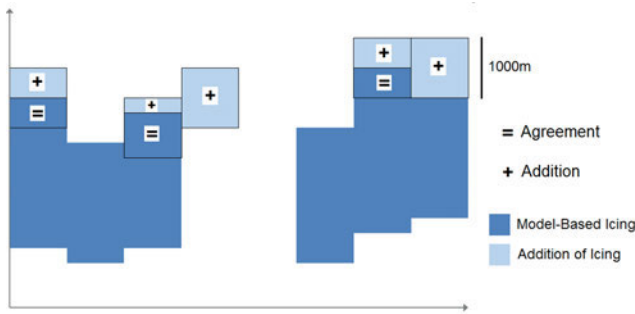
Figure 7: Addition and/or agreement of model-based icing using the combination of CTT, Cloud Phase and Cloud Mask. If there is a cloud whose phase is determined as liquid by the Cloud Phase product and if CTT is between $0\,°C$ and $-20\,°C$, a general icing risk is assigned to sub-freezing cloud layers up to 1000 m below cloud top.

Table 1: Weighting factors w_x for the calculation of icing intensity I as given in Eq. (3.2).

	w_{si}	w_{zsi}	$w_{lwcmodel}$	$w_{lwcparcel}$	$w_{\Delta zconv}$
Scenarios "Stratiform" and "General"	0.2	0.2	0.2	0.2	0.2
Scenario "Convective"	0	0	0	0.75	0.25

Table 2: Empirical thresholds for deriving the three icing intensity levels from the icing intensity scalar I.

Threshold	Icing intensity level
$I = 0$	No icing
$0 < I < 0.4$	Light icing
$0.4 \leq I < 0.7$	Moderate icing
$0.7 \leq I \leq 1.0$	Severe icing

craft structures and is therefore proportional to the supercooled liquid water content SLWC. As mentioned in Section 3.1, the amount and spatial distribution of liquid water output lwc_{model} currently predicted by COSMO-EU is insufficiently realistic. Because of this, additional atmospheric parameters that correlate with SLWC are derived from the COSMO-EU model output to serve as a proxy for SLWC. One of these is the supersaturation with respect to ice that was introduced into ADWICE by LEIFELD (2003). For relative humidity values greater than 100 %, solid ice and supercooled liquid hydrometeors may co-exist until the SLW is depleted by the Bergeron-Findeisen conversion process. Supersaturation with respect to ice is interpreted as indicating the presence of liquid droplets that feed the supersaturation by evaporating. Both the degree s_i and the vertical extent of the supersaturation with respect to ice z_{si} are used, as long as two or more contiguous model layers with this characteristic are found.

In addition to the model derived liquid water output lwc_{model}, an alternate LWC is calculated by a parcel method which provides an adiabatic estimate of the LWC available through vertical transport within the clouds. A detailed description of the parcel method and its corresponding liquid water output lwc_{parcel} is given by TAFFERNER et al. (2003) and is therefore omitted here.

Furthermore, the vertical extent of convective systems Δz_{conv} is calculated. The greater Δz_{conv} is, the more probable is the existence of SLW within these clouds. The calculation of Δz_{conv} was mentioned in Eq. (3.1).

The above mentioned atmospheric parameters are quantitatively correlated with the icing intensity level. A fuzzy logic approach using membership functions (see Figure 8) is applied to transfer the values of atmospheric parameters x into factors F_x with a domain between 0 and 1. A weighting function is then used to combine the factors for calculating the final icing intensity I

$$I = \sum_x w_x F_x, \qquad (3.2)$$

where w_x is a weighting factor given by Table 1.

The previously identified icing scenarios specify which factors are used for the calculation of the icing intensity. Icing areas with the scenario "Freezing" are automatically assigned the maximum icing intensity level "severe" because SLD conditions are almost certain to exist here. Regarding the icing scenarios "Stratiform" and "General", all factors are used with equal weighting w_x for the calculation of the icing intensity (see Table 1). If the "Convective" scenario was identified, the icing intensity is calculated by an alternate weighting function using the parcel method LWC output with a higher weighting and the vertical extent of the convective cloud system with a lower weighting. The resulting scalar I has a domain between 0 and 1 as well. To derive the icing intensity categories, empirical thresholds are applied to this domain, as shown in Table 2.

It has to be considered that this icing intensity calculation is based on atmospheric parameters. It is not possible to derive an aircraft type specific hazard from this value. Furthermore, it should be mentioned that icing intensity depends on the distance the aircraft travels in the icing conditions. Appendix C assumes a standard length of approximately 30 km (17.4 nmi) for stratiform icing. What is predicted here is an icing intensity on a 7 km scale. Therefore, values of LWC for the calculation of icing intensity related to Appendix C should be increased.

3.5 Output data

The output of ADWICE PIA and DIA is a three-dimensional icing product referred to as the Prognostic Icing Product (PIP) and Diagnostic Icing Product (DIP), respectively. Both PIP and DIP provide information about the spatial distribution of the previously introduced icing scenarios and the icing intensity to be expected within these icing conditions. Figure 9 shows a colour-coded graphical output of the PIP in a top-down composite view showing column maxima for 04:00 UTC 06 November 2013. This example
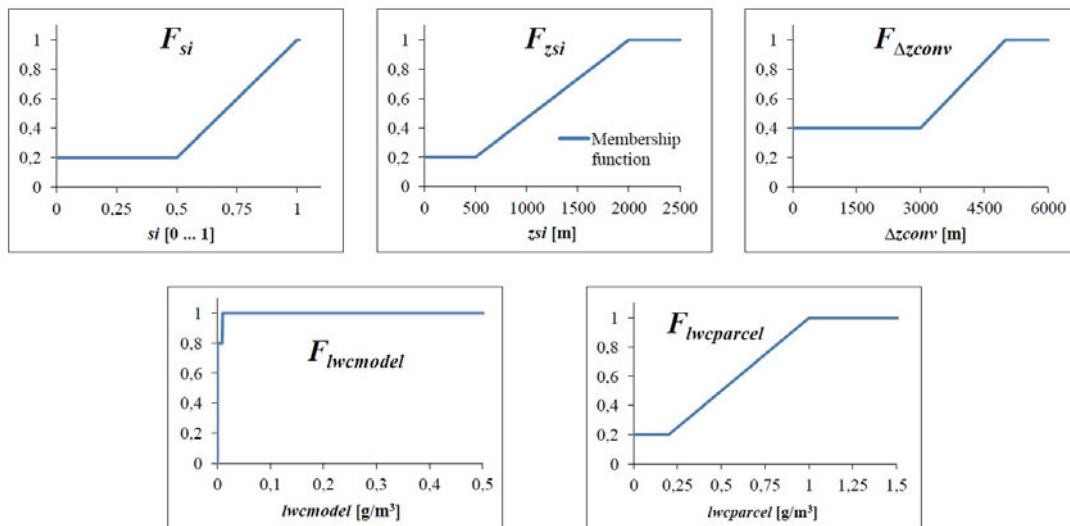
Figure 8: Membership functions F_x for the calculation of icing intensity as given in Eq. (3.2). S_i is the degree, z_{si} the vertical extent of supersaturation with respect to ice, Δz_{conv} the vertical extent of convective clouds (Eq. (3.1)), lwc_{model} the liquid water content derived by the model and lwc_{parcel} the liquid water content derived by the parcel method.
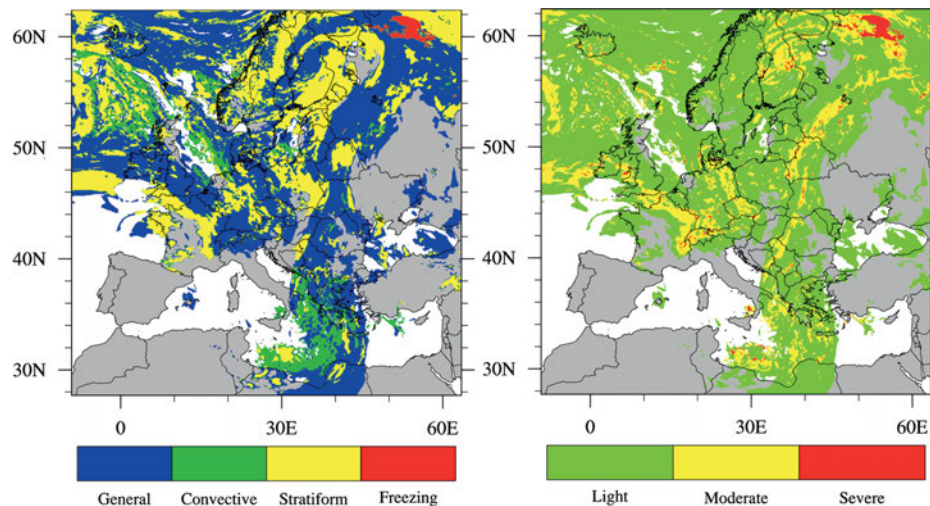

Figure 9: Illustration of the ADWICE output PIP. Left: a composite view presenting the distribution of the four icing scenarios "General" (blue), "Convective" (green), "Stratiform" (yellow) and "Freezing" (red). Right: the associated icing intensity within the three intensity levels "Light" (green), "Moderate" (yellow) and "Severe" (red).

case demonstrates that ADWICE is capable of resolving also small-scale icing conditions, e.g., within a cluster of thunderstorms to the northeast of Sicily which were verified by a pilot reporting moderate icing conditions in this area.

PIA runs operationally at DWD and is updated four times a day at about 03, 09, 15 and 21 UTC following the main runs of COSMO-EU at 00, 06, 12 and 18 UTC. PIA provides an hourly forecast 21 hours ahead (00/06/12/18 UTC + 4 h, + 5 h, ..., 24 h), followed by a three-hourly forecast between the forecast times +24 h and +48 h, followed by a six-hourly forecast between the forecast times +48 h and +78 h. In contrast, DIA runs every hour based on the current PIP and all necessary observational data. PIP and DIP are both available across 30 model layers and interpolated to 12 flight levels.

4　Verification against pilot reports over Europe

A validation study was performed to quantify the impact of the above described implementation of satellite derived data in ADWICE-DIA. For this purpose, the prognostic and the diagnostic icing products (with and without implemented satellite data) are separately compared with pilot reports.

4.1　Validation data and quality

PIREPS currently represents the only widely available dataset for direct in-situ icing observations aloft that can identify the existence of supercooled liquid water in the atmosphere. However, over Europe there are some problematic properties that must be considered:

- Pilot observed icing intensity is subjective and is defined by the impact on aircraft handling, which depends, e.g., on the size and speed of the aircraft, the angle of attack, the aircraft de-icing system on board, if any, and on other factors. Severe icing for a small sports airplane without any de-icing system may be regarded as trace ice for bigger airplanes with heated wings. The severity of reported icing is insufficiently defined to compare directly with model-derived icing intensity. For this reason, all observed icing degrees light, moderate and severe are summarised in the following evaluation as a positive observation ("YES").
- PIREPS are human-based. If a pilot notices ice accumulation, countermeasures (activation of de-icing, descending or climbing, etc.) have to be initiated first. In general, the report is transmitted as soon as the aircraft is in a less stressful situation for the pilot, thus allowing him to report the event to the ground. Altogether, this results in time delays and an inaccurate horizontal and vertical location of the observed event.
- The transmission of a PIREP is requested of pilots but is not obligatory, so that not all events are reported.
- "No icing" is rarely reported. However, negative observations are essential for validation studies. To increase the dataset of "no icing events", a PIREP reporting "clear above" is handled as an implicit "no icing" report for the cloud-free area above.
- In summary, PIREPs exhibit strong category bias towards positive events and distribution bias around icing areas. On top of this, PIREPs are also naturally biased in their distribution towards areas of high air traffic density.

PIREPs over Europe are often signed by hand and afterwards not transmitted to the meteorological offices. There is no centralised and unified European collection system so that data are easily lost or even not transmitted because of time constraints, depending on the weather situation. Nevertheless, the PIREP data is currently the only source to verify forecasting systems for in-flight icing. The validation study presented here required the comparison of point observations (PIREPs) with point forecast/diagnosis values derived from the gridded ADWICE output. In order to consider inaccuracies in space and time in the observations as well as in the model output, the required point value for the forecast/diagnosis was not simply taken from the grid point closest to the observation, but rather generated from several grid points around the observation. The maximum of predicted and diagnosed icing in a generated cube of 7×7 horizontal and three vertical model grid boxes (approximately 49×49 km in horizontal; vertical distance depends on the level and surface height: the closer to the surface, the lower the distance in between the levels, and vice versa) was compared with the PIREP information. For time consideration, always the next forecast hour to the observational time according to Section 3.5

Table 3: Skill scores "Hit", "False Alarm", "Miss" and "Correct Rejection".

		Observation	
		Yes	*No*
Forecast	*Yes*	Hit (H)	False Alarm (FA)
	No	Miss (M)	Correct Rejection (CR)

was taken (for example, if the PIREP was observed at 07:35 UTC, PIA from 00 UTC run + 08 h and observational data from 08 UTC have been used). If there is any positive forecasted or diagnosed grid box in the generated cube, the whole cube is set to "positive". No icing in the cube can therefore only occur, if all grid boxes within have the value of zero.

4.2 Probability of detection

In this verification study, observational data is compared with the generated values, from the model cube as described in Section 4.1, by using a contingency table calculating the probability of detection (see also Table 3).

Cases where both forecast and observation have a "yes" (yes/yes) value are called a "Hit" (H), meaning that the occurrence of an event was correctly predicted/diagnosed. Cases where the forecast or diagnosis contain a "yes" value, but the observation a "no" (yes/no) are called a "False Alarm" (FA). If the forecast contains a "no", but the observation is "yes", then this is called a "Miss" (M). If both observation and forecast are "no", it is called a "Correct Rejection" (CR).

The probability of detection (POD) must then be divided into two parts, POD_{yes} and POD_{no}, because the strong biases and unsystematic nature of the observations allow no cross-column statistical measures. POD_{yes} is the fraction of correctly predicted/diagnosed events out of all positive observations (Hit Rate) and is calculated by

$$POD_{yes} = \frac{H}{H + M}. \quad (4.1)$$

POD_{no} is calculated by

$$POD_{no} = \frac{CR}{CR + FA} \quad (4.2)$$

and describes the fraction of correct rejections out of all negative observations. Values of POD_{yes} and POD_{no} are in between zero (0 %) and one (100 %), where zero denotes a completely incorrect forecast/diagnosis and inversely, a value of one denotes a perfect forecast/diagnosis.

4.3 Area under curve

Plotting $1 - POD_{no}$ on the x-axis and POD_{yes} on the y-axis leads to the Receiver Operating Characteristic (ROC) curve. It is a 2D graph and describes the Hit Rate against the False Alarm Rate, graphically illustrating

additional characteristics of forecast/diagnosis skill. The curve is plotted beginning in $x = 0$ and $y = 0$, through all POD pairs and ends in $x = 1$ and $y = 1$. The area in between the x-axis and the ROC-curve is called the "Area Under Curve" (AUC), representing a measure of the forecast's ability to discriminate between "yes" and "no" observations. An AUC value of 0.5 represents a random equivalent forecast, values above 0.5 represent a better forecast, values below 0.5 a worse forecast.

4.4 Volume efficiency

PIREPS are usually reported to warn following aircraft in case of any severe weather event. Accordingly, non-severe weather reports are nearly unimportant for flight safety so that they are reported rarely. This low number of data points makes it difficult to determine a reliable true False Alarm Rate for the diagnosis and forecasts of ADWICE. The concept of volume efficiency is therefore used as an alternative, since it can help illustrate the relative amount of spatial-volume different-diagnosis outputs assigned with the icing potential to achieve their hit rate. This relationship between POD_{yes} and the icing volume simulated in a prognosis or diagnosis is described by

$$Vol_{eff} = 100 \cdot \frac{POD_{yes}}{Vol\%}, \qquad (4.3)$$

where the icing volume percentage is defined as

$$Vol\% = 100 \cdot \frac{Vol_{ice}}{Vol_{tot}}. \qquad (4.4)$$

Here, Vol_{ice} is the summed volume of all grid points with an associated positive event and Vol_{tot} is the summed volume of all grid points. The Volume Efficiency sets the values of POD_{yes} in relation to the fraction of total predicted/diagnosed icing. The higher Vol_{eff}, the more reliable POD_{yes}. This approach is therefore very useful in simulations where a reliable POD_{yes} may be calculated from a large number of positive observations, but a low number of negative observations leads to an unreliable POD_{no}. It must be stressed, however, that absolute values for $Vol\%$ and Vol_{eff} are in themselves meaningless and are only useful to illustrate differences in algorithm configurations that run on otherwise identical model grids (constant Vol_{tot}).

4.5 Results

From October 2013 to the end of January 2014, 848 PIREPS with positive and negative icing information were collected over Europe. The geographic distribution is shown in Figure 10. In 824 cases, at least "light icing" was observed, where in only 24 cases, "no icing" or "clear above" were reported. Neglecting the reported icing intensity, every PIREP was compared with its associated "model cube" as described in Section 4.1. The calculated skill scores can be found in Table 4.
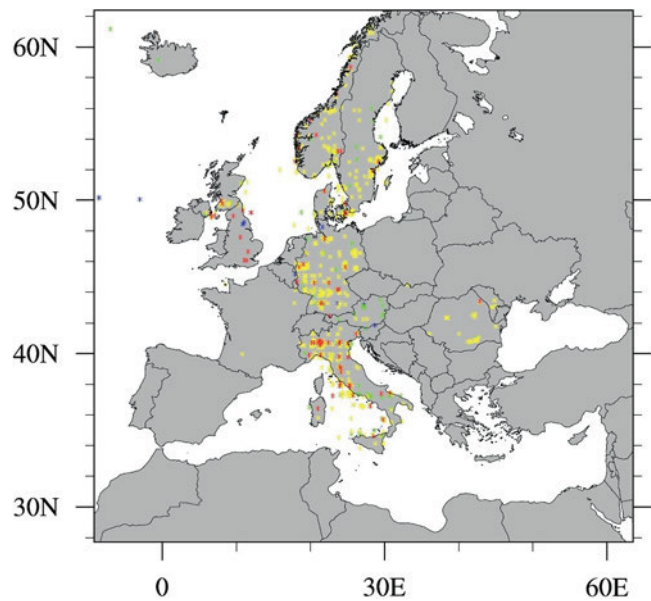

Figure 10: Location of 848 observed PIREPS over Europe between October 2013 and January 2014. Green = light, yellow = moderate, red = severe and blue = no icing observed.

Table 4: Results of PIA and DIA with and without satellite data in comparison with pilot icing observations.

	POD$_{yes}$ (%)	POD$_{no}$ (%)	Vol%	Vol$_{eff}$	AUC
Prognosis	90.78	62.5	12.7	7.14	0.77
Diagnosis, without sat.-data	88.11	62.5	11.4	7.72	0.75
Diagnosis, with sat.-data	88.47	62.5	9.54	9.28	0.75

With nearly 91 %, PIP shows the best results in Hit Rate, whereas DIP, both with and without satellite data, has a slightly lower Hit Rate of ca. 88 %. POD_{no} stays equal in all three runs at 62.5 % due to the low number of 24 "no icing" observations. The corresponding AUC values are 0.77 for PIA and 0.75 for both DIA versions. Initially, it is notable that the Hit Rate does not increase for DIA, even though observational data is used. But filling all model grid points with a positive icing event would lead to a Hit Rate of 100 % as well as to a False Alarm Rate of 100 %. This is the reason why a few negative observations cannot be a reliable basis for finding a significant statistical conclusion about POD_{no} and about the model performance. Due to the lack of negative observations, the Volume Efficiency described in Section 4.4 was introduced to allow a conclusion about model performance: the higher the Volume efficiency, the better the model performance. Results for Volume Efficiency were raised from 7.14 in PIA to 7.72 in DIA without satellite data, and finally to 9.28 in DIA using satellite data. Fewer grid points are assigned icing conditions while the hit rate remains high.

The influence of the individual satellite products as well as of SYNOP and RADAR data on icing diagnosis
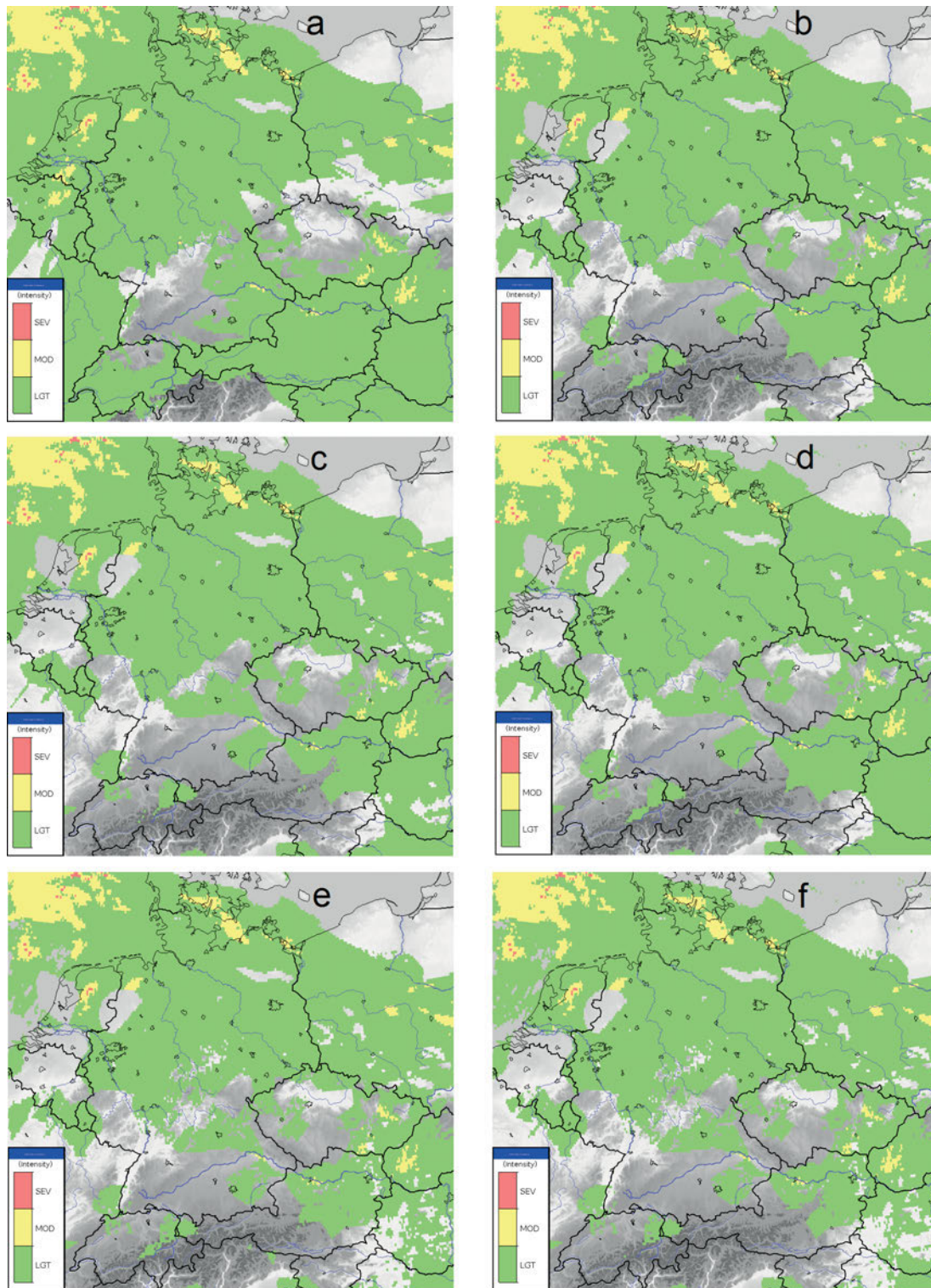
Figure 11: Calculated icing intensities over middle Europe for December, 8th 2016 within the three intensity levels "Light" (green), "Moderate" (yellow) and "Severe" (red) by (a) Prognosis, (b) Diagnosis with SYNOP and RADAR and without Satellite data, (c) as for (b) but with Cloud Mask as icing reduction, (d) as for (b) but with icing addition by Cloud Phase, (e) as for (b) but with reduction by Cloud Top Height and (f) with all ground observations and Satellite data.

for middle Europe are shown in Figure 11a–f for December 8th 2016, 11 UTC. Figure 11a shows the icing intensities of the prognostic algorithm (as described in Section 3.2). An addition of SYNOP and RADAR data on icing prognosis (as described in Sections 3.3.1 and 3.3.2) mainly leads to a slight reduction of areas where icing was formerly prognosed (Figure 11b). Only a few icing grid points were removed by the inclusion of the cloud mask (Figure 11c) and furthermore, added by the usage of CTT, Cloud Phase and Cloud Mask as icing ad-

ditions (see Figure 11d). The highest influence of satellite products has the usage of CTH for icing reduction of model-based icing tops (see Figure 11e). The final result using all ground observations, RADAR and satellite data is shown in Figure 11f.

In conclusion, the newly introduced satellite algorithm in DIA efficiently reduces over-forecasting relative to PIA. Because of the low number of PIREPS over Europe, an additional validation campaign was performed over the United States, where a reliable number of diverse pilot reports exist. Results for POD_{yes} with a value of nearly 90 % are almost similar to those over Europe, whereas POD_{no} (21.5 %) and AUC (0.556) are somewhat lower than over Europe (Tendel 2013). But again, the satellite-based icing product of ADWICE was able to reduce the overall icing volume percentage by between 10 % and 30 %. Furthermore, ADWICE was compared with FIP in Tendel and Wolff (2011). The study found good agreement in fundamental model skill indicated by stable and very similar AUC scores.

5 Conclusions and future work

ADWICE consists of a diagnostic part DIA, which may be seen as a nowcasting system, and a very similar prognostic part PIA where the required observational input data are replaced by or estimated from model output data. The icing diagnosis quality depends on the amount, quality and type of input data. Standard input data includes temperature and specific humidity from a NWP model, as well as SYNOP and METAR information, radar, and satellite data.

In this paper, it was shown how the newly introduced satellite data are implemented in ADWICE and how the overall quality of ADWICE was improved. The main improvement in the use of satellite data brought to ADWICE lies in the reduction of over-diagnosis by allowing the identification of additional icing-free areas in the model domain that were conservatively labelled as potential icing by the baseline algorithm. This reduction in icing volume while maintaining a high rate of correctly capturing reported icing encounters implies a more accurate placement of icing areas. This also increases trust in the diagnosis of no-icing conditions, an important factor for visual flight rules (VFR) flight safety.

The various icing expert systems such as ADWICE, SIGMA (Meteo France) and CIP/FIP (NCAR) are adjusted to the region to which they are applied. Opportunities for optimisation lie in the differences in spatial availability, e.g., for SYNOP data in Europe and in the US and in the weighting with which those data enter the algorithms.

Validation of ADWICE and other icing expert systems is conventionally performed against PIREPs. These have some significant deficiencies as validation data, but are, so far, the only readily available independent icing information source. Any warning scheme suffers from significant over-forecasting, and correspondingly high false-alarm-rates. To quantify this, negative (no) icing information is needed, which unfortunately is not provided in sufficient quality by PIREPs. This will hopefully change in the future when aircraft data from icing detectors will be included in the AMDAR datalink scheme and will be reported to the ground. PIREPs mostly report positive ("yes") icing information. Icing detector signals will consistently report "no icing" as well. Experience shows that in more than 90 % of all cases, icing conditions are not present in a particular cloud. Systematic icing detector readings will alleviate the category bias and the icing-related location bias of PIREPs and report realistic fractions of icing vs. no-icing conditions along the flight path. The location bias toward areas with a high air-traffic density will remain, however. In the future, PIREPs may continue to be used for validation, as presented in this paper. However, they may also be used as an additional information source in nowcasting systems.

The AMDAR programme will also introduce airborne humidity measurements in the near future. From that data, one may infer the existence of clouds and ice supersaturation. Both measurement quantities would be hugely beneficial in ADWICE and of course in all NWP models.

Besides the AMDAR measurements, other valuable data sources will become operationally available in the future. One of them will be Doppler polarisation radar information and the coupled particle identification algorithm. This will allow, for instance, the direct detection of liquid water vs. ice crystals in precipitation, enabling the remote identification of supercooled freezing rain or inversely, the SLWC depletion potential of ice crystals.

In conclusion, the current ADWICE version has proven to be a successful update to the system for diagnosing supercooled liquid water content. There is, however, still significant room for improvement concerning the detection of SLWC and also of the icing severity. Future data sources, including the improved use of next-generation NWP output will serve to also improve the forecast products.

Acknowledgments

References

Abbat,t J.P.D., S. Benz, D.J. Cziczo, Z.A. Kanji, U. Lohmann, O. Möhler, 2006: Solid Ammonium Sulfate Aerosols as Ice Nuclei: A Pathway for Cirrus Cloud Formation. – Science **313**, 1770–1773. DOI: 10.1126/science.1129726.

Andreae, M.O., D. Rosenfeld, 2008: Aerosol-cloud-precipitation interactions, Part 1: The nature and sources of cloud-active aerosols. – Earth-Sci. Rev. **89**, 13–41. DOI: 10.1016/j.earscirev.2008.03.001.

Appiah-Kubi P., 2011: U.S Inflight Icing Accidents and Incidents, 2006 to 2010. – Master thesis. University of Tennessee, Knoxville.

Bernstein, B.C., C. LeBot, 2009: An Inferred Climatology of Icing Conditions Aloft, Including Supercooled Large Drops. Part II: Europe, Asia, and the Globe. – J. Appl. Meteor. Climatol. **48**, 1503–1526. DOI: 10.1175/2009JAMC2073.1.

Bernstein, B.C., T.A. Omeron, F. McDonough, M.K. Politovich, 1997: The Relationship between Aircraft Icing and Synoptic-Scale Weather Conditions. – Wea. Forecast. **12**, 742–762. DOI: 10.1175/1520-0434(1997)012<0742:TRBAIA>2.0.CO;2.

Bernstein, B.C., F. McDonough, M.K. Politovich, B.G. Brown, 2005: Current Icing Potential: Algorithm Description and Comparison with Aircraft Observations. – J. Appl. Meteor. **44**, 969–986. DOI: 10.1175/JAM2246.1.

Bernstein, B.C., C.A. Wolff, F. McDonough, 2007: An Inferred Climatology of Icing Conditions Aloft, Including Supercooled Large Drops. Part I: Canada and the Continental United States. – J. Appl. Meteor. Climatol. **46**, 1857–1878. DOI: 10.1175/2007JAMC1607.1.

Christner, B.C., C.E. Morris, C.M. Foreman, R. Cai, D.C. Sands, 2008: Ubiquity of Biological Ice Nucleators in Snowfall. – Science **319**, 1214. DOI: 10.1126/science.1149757.

Cober, S.G., G.A. Isaac, 2012: Characterization of Aircraft Icing Environments with Supercooled Large Drops for Application to Commercial Aircraft Certification. – J. Appl. Meteor. Climatol. **51**, 265–284. DOI: 10.1175/JAMC-D-11-022.1.

DeBerg, M., M. vanKreveld, M. Overmars, O. Schwarzkopf, 2000: Voronoi Diagrams. – Computational Geometry: Algorithms and Applications, Springer **7**, 147–163.

DeMott, P.J., D.J. Cziczo, A.J. Prenni, D.M. Murphy, S.M. Kreidenweis, D.S. Thomson, R. Borys, D.C. Rogers, 2003: Measurements of the concentration and composition of nuclei for cirrus formation. – Proceedings of the National Academy of Sciences of the United States of America **100**, 14655–14660.

DeMott, P.J. and Coauthors, 2011: Resurgence in Ice Nuclei Measurement Research. – Bull. Amer. Meteor. Soc. **92**, 1623–1635. DOI: 10.1175/2011BAMS3119.1.

Doms, G., 2011: A Description of the Nonhydrostatic Regional COSMO – Model. Part I: Dynamics and Numerics. – Technical Report, Deutscher Wetterdienst, Offenbach, Germany, 153 pp.

Doms, G., J. Förstner, E. Heise, H-J. Herzog, D. Mironov, M. Raschendorfer, T. Reinhardt, B. Ritter, R. Schrodin, J-P. Schulz, G. Vogel, 2011: A Description of the Nonhydrostatic Regional COSMO – Model. Part II: Physical Parameterizations. – Technical Report, Deutscher Wetterdienst, Offenbach, Germany, 161 pp.

Flossmann, A.I., W. Wobrock, 2010: A review of our understanding of the aerosol cloud interaction from the perspective of a bin resolved cloud scale modelling. – J. Atmos. Res. **97(4)**, 478–497. DOI: 10.1016/j.atmosres.2010.05.008.

Forbes, G.S., Y. Hu, B.G. Brown, B.C.. Bernstein, M.K. Politovic, 1993: Examination of conditions in the proximity of pilot reports of icing during STORM-FEST. – Fifth International Conference on Aviation Weather Systems. 2–6 August 1993, Vienna, Virginia, American Meteorological Society, 282-286.

Green S.D., 2006: A study of U.S. Inflight Icing Accidents, 1978 to 2002. – Proceedings of the 44th AIAA Aerospace Sciences Meeting and Exhibit, AIAA 2006-82, Reno, Nevada.

Hauf, T., F. Schröder, 2006: Aircraft icing research flights in embedded convection. – Meteorology and Atmospheric Physics **91**, 247–265. DOI: 10.1007/s00703-004-0082-y.

Hedde, T., D. Guffond, 1995: ONERA Three-Dimensional Icing Model. – AIAA Journal **33**, 1038–1045.

Hung, H.M., A. Malinowski, S.T. Martin, 2003: Kinetics of Heterogeneous Ice Nucleation on the Surfaces of Mineral Dust Cores Inserted into Aqueous Ammonium Sulfate Particles. – J. Phys. Chem. **A 107**, 1296–1306. DOI: 10.1021/jp021593y.

Isaac, G.A., S.J. Cober, J.W. Strapp, A.V. Korolev, A. Tremblay, D.L. Marcotte, 2001: Recent Canadian research on aircraft in-flight icing. – Canadian Aeronautics Space J. **47**, 213–221.

Jeck, R.K., 2002: Icing Design Envelopes (14 CFR Parts 25 and 29, Appendix C) Converted to a Distance-Based Format. DOT/FAA/AR-00/30. Federal Aviation Administration, Airport and Aircraft Safety Research and Development, William J. Hughes Technical Center, Atlantic City International Airport, NJ 08405. Final Report, available to the U.S. public through the National Technical Information Service (NTIS), Springfield, Virginia 22161a.

Kärcher, B., O. Möhler, P.J.. DeMott, S. Pechtl, F. Yu, 2007: Insights into the role of soot aerosols in cirrus cloud formation. – J. Atmos. Chem. Phys. **7**, 4203–4227. DOI: 10.5194/acp-7-4203-2007.

Köhler, F., U. Görsdorf, 2014: Towards 3D prediction of supercooled liquid water for aircraft icing: Modifications of the microphysics in COSMO-EU. – Meteorol. Z. **23**, 253–262. DOI: 10.1127/metz/2014/0545.

Korolev, A.V., G.A. Isaac, S.G. Cober, J.W. Strapp, J. Hallett, 2003: Microphysical characterization of mixed-phase clouds. – Quart. J. Roy. Meteor. Soc. **129**, 39–65. DOI: 10.1256/qj.01.204.

LeBot, C., 2003: SIGMA: System of Icing Geographic identification in Meteorology for Aviation. – SAE Technical Paper. DOI: 10.4271/2003-01-2085.

Leifeld C., 2003: Weiterentwicklung des Nowcastingsystems ADWICE zur Erkennung vereisungsgefährdeter Lufträume. – PhD thesis. Institute of Meteorology and Climatology, Gottfried Wilhelm Leibniz Universität Hannover, Hannover, Germany, 113 pp.

Lohmann, U., K. Diehl, 2006: Sensitivity Studies of the Importance of Dust Ice Nuclei for the Indirect Aerosol Effect on Stratiform Mixed-Phase Clouds. – J. Atmos. Sci. **63**, 968–982. DOI: 10.1175/JAS3662.1.

Martin S.T., 1998: Phase transformations of the ternary system (NH4)2SO4-H2SO4-H2O and the implications for cirrus cloud formation. – Geophys. Res. Lett. **25**, 1657–1660.

Marwitz, J.D., M.K. Politovich, B.C. Bernstein, F.M. Ralph, P.J. Neiman, R. Ashenden, J. Bresch, 1997: Meteorological Conditions Associated with the ATR-72 Aircraft Accident near Roselawn, Indiana on 31 October 1994. – Bull. Amer. Meteor. Soc. **78**, 41–52. DOI: 10.1175/1520-0477(1997)078<0041:MCAWTA>2.0.CO;2

McDonough, F., B.C. Bernstein, 1999: Combining satellite, radar and surface observations with model data to create a better aircraft icing diagnosis. – Proceedings of the 8th Conference on Aviation, Range and Aerospace Meteorology. 10–15 January 1999, Dallas, TX, 467–471.

Miller D., T. Ratvasky, B.C. Bernstein, F. McDonough, J.W. Strapp, 1998: NASA/FAA/NCAR supercooled large droplet icing flight research: summary of winter 96/97 flight operations. – Proceedings of 36th Aerospace Science Meeting and Exhibit, AIAA, Reno, NV, 12–15 January 1998. DOI: 10.2514/6.1998-577.

Möhler, O., P.J. DeMott, G. Vali, Z. Levin, 2007: Microbiology and atmospheric processes: the role of biological particles in cloud physics. – Biogeosci. Discuss. **4**, 2559–2591.

Morrison, H., J.O. Pinto, 2005: Mesoscale Modeling of Springtime Arctic Mixed-Phase Stratiform Clouds Using a

New Two-Moment Bulk Microphysics Scheme. – J. Atmos. Sci. **62**, 3683–3704. DOI: 10.1175/JAS3564.1.

PHILLIPS, V.T.J., T.W. CHOULARTON, A.M. BLYTH, J. LATHAM, 2002: The influence of aerosol concentrations on the glaciation and precipitation of a cumulus cloud. – Quart. J. Roy. Meteor. Soc. **128**), 951–971. DOI: 10.1256/0035900021643601.

POLITOVICH, M.K., 1996: Response of a Research Aircraft to Icing and Evaluation of Severity Indices. – Journal of Aircraft, **33(2)**, 291–297. DOI: 10.2514/3.46936.

POLITOVICH, M.K., 2000: Predicting Glaze or Rime Ice Growth on Airfoils. – J. Aircraft **37**, 117–121. DOI: 10.2514/2.2570.

POLITOVICH, M.K., B.C. BERNSTEIN, 1995: Production and depletion of supercooled liquid water in a Colorado winter storm. – J. Appl. Meteor. **34**, 2631–2648. DOI: 10.1175/1520-0450(1995)034<2631:PADOSL>2.0.CO;2.

POLITOVICH, M.K., A.O. TIFFANY, B.C. BERNSTEIN, 2002: Aircraft Icing Conditions in Northeast Colorado. – J. Appl. Meteor. **41**, 118–132.

PRUPPACHER, H.R., J.D. KLETT, 1997: Microphysics of Clouds and Precipitation, – Kluwer Academic Publishers, Dordrecht, 954 pp.

RASMUSSEN, R.M., M. POLITOVICH, W. SAND, G. STOSSMEISTER, B.C. BERNSTEIN, K. ELMORE, J. MARWITZ, J. McGINLEY, J. SMART, E. WESTWATER, B. STANKOV, R. PIELKE, S. RUTLEDGE, D. WESLEY, N. POWELL, D. BURROWS, 1992: Winter icing and storms project (WISP). – Bull. Amer. Meteor. Soc. **73.**, 951–974. DOI: 10.1175/1520-0477(1992)073<0951:WIASP>2.0.CO;2.

RASMUSSEN, R.M., B.C. BERNSTEIN, M. MURAKAMI, G. STOSSMEISTER, J. REISNER, B. STANKOV, 1995: The 1990 Valentine's Day arctic outbreak. Part I: Mesoscale and microscale structure and evolution of a Colorado Front Range shallow upslope cloud. – J. Appl. Meteor. **34**, 1481–1511. DOI: 10.1175/1520-0450-34.7.1481.

ROLOFF, K., 2012: Untersuchung zur Eignung wolkenmikrophysikalischer Parameter des numerischen Wettervorhersagemodells COSMO-EU zur Vereisungsprognose in ADWICE. – Master thesis. Institute of Meteorology and Climatology, Gottfried Wilhelm Leibniz Universität Hannover, Hannover, Germany, 141 pp.

ROSENFELD, D., W.L. WOODLEY, 2000: Deep convective clouds with sustained supercooled liquid water down to $-37.5\,°C$. – Nature **405**, 440–442. DOI: 10.1038/35013030.

ROSENFELD, D., R. CHEMKE, P. DEMOTT, R.C. SULLIVAN, R. RASMUSSEN, F. McDONOUGH, J. COMSTOCK, B. SCHMID, J. TOMLINSON, H. JONSSON, K. SUSKI, A. CAZORLA, K. PRATHER, 2013: The common occurrence of highly supercooled drizzle and rain near the coastal regions of the western United States. – J. Geophys. Res. Atmos. **118**, 9819–9833. DOI: 10.1002/jgrd.50529.

RUFF, G.A., M. BERKOWITZ, 1990: Users Manual for the NASA Lewis Ice Accretion Prediction Code (LEWICE). – NASA Contractor Report 185129.

RYERSON, C., G. KOENIG, F. SCOTT, 2000: Retrieval of cloud microphysics during the Mt. Washington Icing Sensors Project (MWISP). – Proceedings of the 8th Conference on Aviation, Range and Aerospace Meteorology, Orlando, FL, 531–535.

SCHULTZ, P., M.K. POLITOVICH, 1992: Toward the Improvement of Aircraft Icing Forecasts for the Continental United States. – Wea. Forecast. **7**, 491–500. DOI: 10.1175/1520-0434(1992)007<0491:TTIOAI>2.0.CO;2.

SHILLING, J.E., T.J. FORTIN, M.A. TOLBERT, 2006: Depositional ice nucleation on crystalline organic and inorganic solids. – J. Geophys. Res. Atmos. **111**, DOI: 10.1029/2005JD006664.

TAFFERNER, A., T. HAUF, C. LEIFELD, T. HAFNER, H. LEYKAUF, U. VOIGT, 2003: ADWICE: Advanced Diagnosis and Warning System for Aircraft Icing Environments. – Wea. Forecast. **18**, 184–203. DOI: 10.1175/1520-0434(2003)018<0184:AADAWS>2.0.CO;2.

TENDEL J., 2013: Warning of In-Flight Icing Risk through Fusion of Satellite Products, Ground Observations and Model Forecasts. – PhD thesis. Institute of Meteorology and Climatology, Gottfried Wilhelm Leibniz Universität Hannover, Hannover, Germany.

TENDEL, J., C. WOLFF, 2011: Verification of ADWICE Inflight Icing Forecasts: Performance vs. PIREPs Compared to FIP. – Proceedings of SAE International Conference on Aircraft and Engine Icing and Ground Deicing, Chicago, IL, June 13–17, 2011. SAE International, Warrendale, PA. DOI: 10.4271/2011-38-0068.

THOMPSON, J., 2012: High-resolution winter simulations over the Colorado Rockies: Sensitivity to microphysics parameterizations. – ECMWF workshop on parameterization of clouds and precipitation across model resolutions. 5-8 November 2012, ECMWF, Reading UK.

THOMPSON, G., R.T. BRUINTJES, B.G. BROWN, F. HAGE, 1997: Intercomparison of In-Flight Icing Algorithms. Part I: WISP94 Real-Time Icing Prediction and Evaluation Program. – Wea. Forecast. **12**, 878–889. DOI: 10.1175/1520-0434(1997)012<0878:IOIFIA>2.0.CO;2.

TIEDTKE, M., 1989: A comprehensive mass flux scheme for cumulus parameterization in large-scale models. – Mon. Wea. Rev. **117**, 1779–1800. DOI: 10.1175/1520-0493(1989)117<1779:ACMFSF>2.0.CO;2.

TRAN, P., M.T. BRAHIMI, I. PARASCHIVOIU, 1995: Ice Accretion on Aircraft Wings with Thermodynamic Effects. – J. Aircraft **32**, 444–446. DOI: 10.2514/3.46737.

WISE, M.E., K.J. BAUSTIAN, M.A. TOLBERT, 2010: Internally mixed sulfate and organic particles as potential ice nuclei in the tropical tropopause region. – Proceedings of the National Academy of Sciences of the United States of America **107(15)**, 6693-6698.

ZUBERI, B., A.K. BERTRAM, C.A. CASSA, L.T. MOLINA, M.J. MOLINA, 2002: Heterogeneous nucleation of ice in $(NH4)2SO4-H2O$ particles with mineral dust immersions. – Geophys. Res. Lett. **29**, 1421–1424. DOI: 10.1029/2001GL014289.